International Journal of Thermophysics, Vol. 27, No. 1, January 2006 (© 2006)
DOI: 10.1007/s10765-006-0022-9

Surface and Size Effects on the Specific Heat Capacity of Nanoparticles[1]

Bu-Xuan Wang,[2,3] Le-Ping Zhou,[2] and Xiao-Feng Peng[2]

Extending the elastic continuum model for fine particles, a theoretical model was proposed to include the different contributions of interior and surface atoms for the specific heat capacity. The effect of size and temperature and the softening of surface atom vibrations were studied, and a dimensionless variable was proposed to characterize the effect of particle size and temperature on the specific heat capacity of nanoparticles. The proposed model was used to fit experimental data for copper oxide nanoparticles.

KEY WORDS: nanoparticle; size effect; specific heat capacity; surface effect.

1. INTRODUCTION

A novel enhancing heat transfer fluid has been proposed recently with nano-sized particles suspended in a liquid, designated as a "nanofluid," to improve obviously the effective thermal conductivity [1]. As a new trial, we have reported our experiments based on a quasi-steady-state principle to measure simultaneously the effective thermal conductivity and specific heat capacity for liquids with nanoparticles suspensions (nanofluid) [2]. For a thermodynamic property, the effective specific heat capacity of a liquid-particle mixture, $C_{v,\mathrm{eff}}$, could be usually treated as the sum of the specific heat capacities for particles, $C_{v,p}$, and for the hosting liquid, $C_{v,l}$, using their respective volume fractions.

[1] Paper presented at the Seventh Asian Thermophysical Properties Conference, August 23–28, 2004, Hefei and Huangshan, Anhui, P. R. China.

[2] Thermal Engineering Department, Tsinghua University, Beijing 100084, P. R. China.
[3] To whom correspondence should be addressed. E-mail: bxwang@mail.tsinghua.edu.cn

Planck [3] firstly pointed out that the phonon spectrum will change from continuous to discrete and the Debye T^3 rule will not be applicable, when the size of the solid particles is sufficiently small. Using the Debye theory, Jura and Pitzer [4] treated nanoparticles as isolated molecules and analyzed the effect of temperature and size on the specific heat capacity of aluminum nanoparticles. Novotny et al. [5] measured the specific heat capacity of lead nanoparticles with different diameters, and proposed that an additional vibration mode of surface phonons will appear at low temperatures and that the size effect on specific heat capacity enhancement of lead nanoparticles will appear at low temperatures. With free boundary conditions and a scalar wave equation of phonons, Baltes and Hilf [6] summed over all vibration modes of phonons in lead nanoparticles to explain the experimental data of Novotny et al. [5] at low temperatures. Lautenschleger [7] alternatively pointed out the size effect on the effective sound velocity and the specific heat capacity of nanoparticles and that the Debye temperature can be expressed as the function of the effective sound velocity, which can be used to study the size effect on the maximum specific heat capacity enhancement of lead nanoparticles using the free boundary condition proposed by Baltes and Hilf [6]. Comsa et al. [8] studied theoretically the specific heat capacity of palladium nanoparticles according to Lautenschleger's method and explained successfully their experimental data for palladium nanoparticles. However, Nishiguchi and Sakuma [9] believed that the scalar wave equation should be replaced by a vector one, and calculated a variation of the specific heat capacity of lead nanoparticles with temperature using the elastic continuum assumption, and they pointed out that the elastic continuum assumption will still be applicable for nanoparticles with diameters larger than 50 Å.

Recently, Zhang and Banfield [10] pointed out that the Einstein and Debye vibration modes of surface and interior atoms in ultra-fine particles are different, and believed that the specific heat capacity of nanoparticles can be expressed as a weighted summation of Einstein and Debye vibration modes. Experimental data of silver and rutile nanoparticles were successfully explained by this assumption. In addition, Prasher and Phelan [11] considered the size effect on the specific heat capacity of nanoparticles to be a function of a dimensionless variable, $R = NT/\theta_D$, and obtained the relation, $C_{P,\mathrm{Micro}}/C_{P,\mathrm{Bulk}} = f(R)$, where $C_{P,\mathrm{Micro}}$ is the specific heat capacity of nanoparticles at constant pressure and $C_{P,\mathrm{Bulk}}$ is the bulk value of the specific heat capacity of the corresponding material, N is the number of atoms in a nanoparticle, T is the temperature, and θ_D is the Debye temperature of the bulk material.

In general, the phonon spectrum is discrete in a nanoparticle, and the contribution of surface phonons to the specific heat capacity of a

nanoparticle cannot be neglected. Thus, starting from the elastic continuum assumption, we will consider in this paper the different contributions of surface and interior atoms to the specific heat capacity of a nanoparticle and calculate the specific heat capacity of a nanoparticle with the Einstein and Debye models, respectively, to study the size and surface effects on the specific heat capacity of a nanoparticle.

2. THEORIES OF LATTICE VIBRATION AND SPECIFIC HEAT CAPACITY

Provided that the base vectors of a primitive cell in a nanoparticle are $\vec{a}_1$, $\vec{a}_2$ and $\vec{a}_3$ the number of primitive cells along the directions of the base vector are N_1, N_2, and N_3, respectively, or the total number of primitive cells is $N = N_1 N_2 N_3$, and there are n different atoms in each primitive cell. Then, using the periodical condition proposed by Born-von Karman, the lattice vibration can be expressed as an elastic wave with $\vec{q}$ as a wave vector [12], or

$$\vec{q} = \frac{l_1}{N_1}\vec{b}_1 + \frac{l_2}{N_2}\vec{b}_2 + \frac{l_3}{N_3}\vec{b}_3, \tag{1}$$

where l_1, l_2, and l_3 are integrals, $\vec{b}_1$, $\vec{b}_2$ and $\vec{b}_3$ are base vectors of a reciprocal lattice primitive cell, and the relation between $\vec{b}_1$, $\vec{b}_2$ and $\vec{b}_3$ and $\vec{a}_1$, $\vec{a}_2$ and $\vec{a}_3$ is

$$\vec{b}_1 = \frac{2\pi(\vec{a}_2 \times \vec{a}_3)}{\Omega}, \quad \vec{b}_2 = \frac{2\pi(\vec{a}_3 \times \vec{a}_1)}{\Omega}, \quad \vec{b}_3 = \frac{2\pi(\vec{a}_1 \times \vec{a}_2)}{\Omega}, \tag{2}$$

where $\Omega = \vec{a}_1 \cdot (\vec{a}_2 \times \vec{a}_3)$ is the volume of a primitive cell. Equations (1) and (2) show that the wave vectors are discrete, the base vectors of a wave vector are $\vec{b}_1/N_1$, $\vec{b}_2/N_2$, and $\vec{b}_3/N_3$, and a single wave vector stands for a repetitive unit, or a reciprocal lattice primitive cell. Due to the periodicity of wave vectors, the wave vectors are usually limited within a reciprocal lattice primitive cell, or the first Brillouin zone; thus, the constraints on wave vectors is

$$-(N_i/2) < l_i \leqslant (N_i/2), \quad (i = 1, 2, 3). \tag{3}$$

The total number of wave vectors is N, and each wave vector corresponds to three acoustic phonons and $(3n - 3)$ photonic phonons; thus, the total number of phonon vibrations is $3nN$.

The phonon is considered to be the quantum of energy of lattice vibrations. Quantum theory has shown that lattice vibrations are equal to the vibrations of $3nN$ phonons, so the phonon vibration energy of a crystal with mass ρV is [12]

$$E = \sum_{\vec{q},p} \frac{\hbar\omega_{\vec{q},p}}{e^{\hbar\omega_{\vec{q},p}/k_B T} - 1}, \tag{4}$$

where ρ is the density of the crystal, $V = N\Omega$ is the volume of the crystal, $\hbar = h/(2\pi)$, h is Planck's constant ($6.626 \times 10^{-34}\,\mathrm{J \cdot s}$), k_B is Boltzmann's constant ($1.381 \times 10^{-23}\,\mathrm{J \cdot K^{-1}}$), T is the temperature, $\omega_{\vec{q},p}$ is the angular frequency of phonon vibrations for a wave vector $\vec{q}$, p is the phonon vibration mode, $p = A$ corresponds to acoustic phonons, and $p = 0$ corresponds to photonic phonons. Using the relation between the specific heat capacity at constant pressure and the energy, the following expression for the volumetric specific heat capacity can be obtained:

$$C_V = \frac{1}{\rho V k_B T^2} \sum_{\vec{q},p} \frac{(\hbar\omega_{\vec{q},p})^2 e^{\hbar\omega_{\vec{q},p}/k_B T}}{(e^{\hbar\omega_{\vec{q},p}/k_B T} - 1)^2}. \tag{5}$$

The specific heat capacity can be calculated by Eq. (5) once the dispersion relation, $\omega = \omega(\vec{q})$, is established.

3. SPECIFIC HEAT CAPACITY OF NANOPARTICLES

The specific heat capacity of a nonmetallic nanoparticle relates only to phonon vibrations; thus, the key factor in calculating the specific heat capacity is to establish the dispersion relation, $\omega = \omega(\vec{q})$. Since the establishment of the dispersion relation is very difficult for three-dimensional phonon vibrations, approximations [12] are usually adapted for describing it. Einstein first proposed an approximation model, and believed that all phonons have the same angular frequency, ω_E. It successfully explained why the low temperature specific heat capacity tends to zero for solids, but it fails to illustrate the T^3 rule when the temperature is approaching zero. Debye assumed that the crystal lattice is a homogenous and continuous medium, and explained successfully the T^3 rule using the simplified linear dispersion relation, or

$$\omega = vq, \tag{6}$$

where v is the effective sound velocity in the medium. Provided that the first Brillouin zone can be approximated to be a spheroid, then v can be determined by

$$v = (\mathrm{k_B}\theta_D/\hbar)/(6\pi^2/\Omega)^{1/3}, \tag{7}$$

where θ_D is the Debye temperature of the bulk material. Then, ω_E can be obtained from the specific heat capacity of the bulk material, $C_{V,\mathrm{Bulk}}$, and the Einstein temperature, θ_E, through the following formula:

$$C_{V,\mathrm{Bulk}} = \frac{3nN\mathrm{k_B}}{\rho V}\left(\frac{\theta_E}{T}\right)^2 \frac{e^{\theta_E/T}}{(e^{\theta_E/T}-1)^2}, \tag{8}$$

$$\omega_E = k_\mathrm{B}\theta_E/\hbar. \tag{9}$$

It is worthwhile to mention that the premises of using the Einstein and Debye models are based on the elastic continuum assumption.

As the variation of the vibration frequency of photonic phonons is small, the Einstein model can be used to approximate these photonic phonons; while for acoustic phonons, which correspond to elastic waves in a continuum, the Debye model is applicable for describing these acoustic phonons. At the same time, as the bonding number of surface atoms is smaller than the number of interior atoms, there exists a vibration-softening phenomenon for surface atoms [13]. When the particle size is within a mesoscale limit, the ratio of the number of surface atoms to the total number of atoms will become greater, and thus the contribution of surface atoms to the specific heat capacity must be considered. Provided that the volume of a unit cell occupies all the space in a spherical particle, then the ratio of the number of surface atoms to the total number of atoms can be expressed as

$$x = \frac{N^\mathrm{I}}{N} = \frac{\pi d^2/(|\vec{a_1}\times\vec{a_2}|+|\vec{a_2}\times\vec{a_3}|+|\vec{a_3}\times\vec{a_1}|)/3]}{(\pi d^3/6)/[\vec{a_1}\cdot(\vec{a_2},\times\vec{a_3})]} = \frac{36\pi}{d(b_1+b_2+b_3)}, \tag{10}$$

where d is the diameter of a nanoparticle. For photonic phonons, the mean vibration frequency can be determined by the weighted summation of phonon vibrations of surface and interior atoms, or

$$\bar{\omega}_E = xL\omega_E + (1-x)\omega_E, \tag{11}$$

where $L = \sqrt{Z^S/Z}$ is the softening factor, Z^S is the averaged bonding number of surface atoms, and Z is the bonding number of interior atoms. So, the contribution of $(3n-3)N$ photonic phonons to the specific heat capacity should be

$$C_{V,0} = \frac{(3n-3)N}{\rho V k_B T^2} \frac{(\hbar\overline{\omega}_E)^2 e^{\hbar\overline{\omega}_E/(k_B T)}}{(e^{\hbar\overline{\omega}_E/(k_B T)}-1)^2}. \tag{12}$$

The softening phenomenon also exists in acoustic phonons. From the Debye assumption, the effective sound velocity of surface atoms is $v^S = Lv$; thus, the contribution of $3N$ acoustic phonons to the specific heat capacity should be

$$C_{V,A} = \frac{3}{\rho V k_B T^2} \left(\sum_{\vec{q} \in Q^I} \frac{(\hbar v q)^2 e^{\hbar v q/(k_B T)}}{(e^{\hbar v q/(k_B T)}-1)^2} + \sum_{\vec{q} \in Q^S} \frac{(\hbar L v q)^2 e^{\hbar L v q/(k_B T)}}{(e^{\hbar L v q/(k_B T)}-1)^2} \right)$$

$$Q^I = \{\vec{q} \mid -(N_i^I/2) < l_i \leqslant (N_i^I/2)\}, \quad N_i^I = xN_i, \qquad i = 1,2,3, \tag{13}$$
$$Q^S = Q - Q^I,\ Q = \{\vec{q} \mid -(N_i/2) < l_i \leqslant (N_i/2)\}, \quad i = 1,2,3.$$

The specific heat capacity of a nanoparticle can thus be determined by the following expression:

$$C_V = C_{V,O} + C_{V,A}. \tag{14}$$

4. ANALYSIS AND DISCUSSION

In this section, we will use the proposed model to calculate the specific heat capacity of a CuO nanoparticle. As shown in Fig. 1[14], copper oxide belongs to the class of monoclinic crystals. There are four CuO molecules in each unit cell, and every primitive cell contains two CuO molecules. Each oxygen atom is connected with four copper atoms, and thus forms a distorted tetrahedron; while in the (110) plane in a unit cell, each

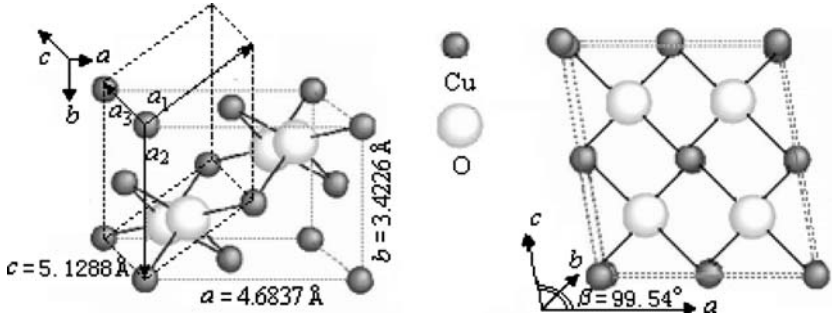

Fig. 1. Unit cell and primitive cell of CuO crystal.

copper atom is bonded with four oxygen atoms, and the links of these oxygen atoms form a quasi-rectangular parallelogram. In the perpendicular plane of this parallelogram, each copper atom is also linked to four oxygen atoms, with longer CuO bonds in this plane. The crystal parameters in a CuO unit cell is measured [14] to be $a = 4.6837$ Å, $b = 3.4226$ Å, $c = 5.1288$ Å, $\alpha = \gamma = 90^\circ$, and $\beta = 99.54^\circ$. The definition of a primitive cell in a CuO crystal is shown in Fig. 1, with the crystal parameters to be $a_1 = 5.8001$ Å, $a_2 = 3.4226$ Å, $a_3 = 5.1288$ Å, $(a_1, a_2) = 111.43^\circ$, $(a_2, a_3) = 90^\circ$, and $(a_3, a_1) = 99.54^\circ$. Thus, the volume of a primitive cell is $\Omega = 41.09$ Å^3, and the base vectors in a reciprocal lattice primitive cell are $\vec{b_1} = 2.6842\,\vec{i}$ Å^{-1}, $\vec{b_2} = 1.3437\,\vec{i} + 1.8367\,\vec{j}$ Å^{-1}, and $\vec{b_3} = 1.2257\,\vec{k}$ Å^{-1}, where the directions of $\vec{i}$ and $\vec{j}$ are parallel to $\vec{a}$ and $\vec{b}$, respectively, and the direction of $\vec{k}$ is perpendicular to the ab plane. For a 50 nm CuO crystal, it is difficult to determine the exact number of primitive cells along the direction of base vectors, so a corresponding cuboid with the same volume is chosen as a substitute for a nanoparticle. If the corresponding cuboid is a cube, then the length of a border will be 40.3 nm, thus $N_1 = 117$, $N_2 = 117$, $N_3 = 117$, and $N = 1,601,613$. An analogous method can be used when determining the numbers of primitive cells along the directions of base vectors.

Figure 2 shows the calculated dispersion relation of acoustic phonons for a 50 nm CuO crystal. It shows that the contribution of surface atoms

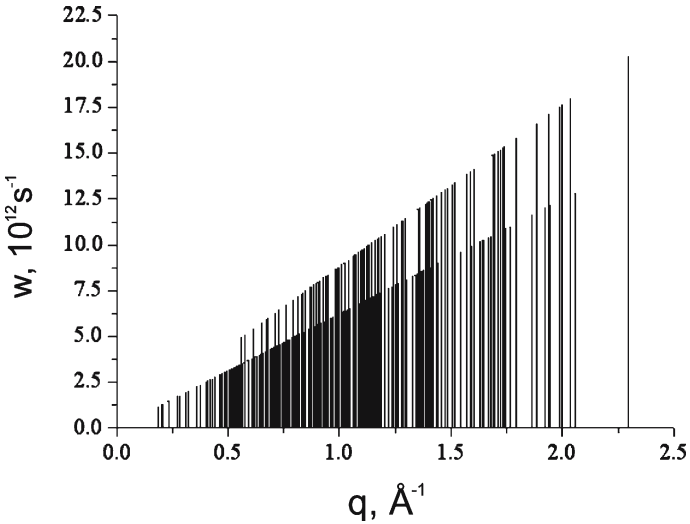

Fig. 2. Dispersion relation of acoustic phonons (50 nm CuO).

to the specific heat capacity cannot be neglected. At the same time, there exists a minimum vibration frequency for acoustic phonons due to a size effect, which is consistent with the conclusion of Nishiguchi and Sakuma [9]. Figure 3 shows the variation of the specific heat capacity for a 50 nm CuO crystal with temperature and the contributions of acoustic and photonic phonons to the specific heat capacity. It can be seen that the specific heat capacity, especially at temperatures less than 225 K, can be considered to be the sum of the Debye and Einstein specific heat capacities; thus, we have successfully explained the assumption that Zhang and Banfield [10] had made in their model.

4.1. Effect of Particle Shape

It is necessary to study the variation of the specific heat capacity when the numbers of primitive cells are changing along the direction of base vectors, since we have made the assumption of an equivalent cuboid. Taking 50 nm and 12.5 nm CuO crystals as examples, the results in Fig. 4a show that the particle shape, for a cubic ($N_1 = N_2 = N_3 = 117$) and others indicated in Fig. 4b, do not affect the specific heat capacity appreciably. The variation of the specific heat capacity for CuO nanoparticles of different diameters with temperature at higher temperatures is shown in Fig. 4b, where the multiplying numbers stand for the number of primitive cells along the directions of base vectors. It can be seen that the value of the specific heat capacity of cubic and thin particles are higher than for the

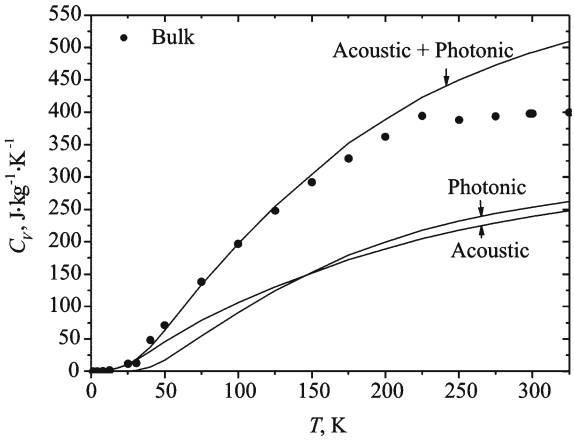

Fig. 3. Specific heat capacity of 50 nm CuO.

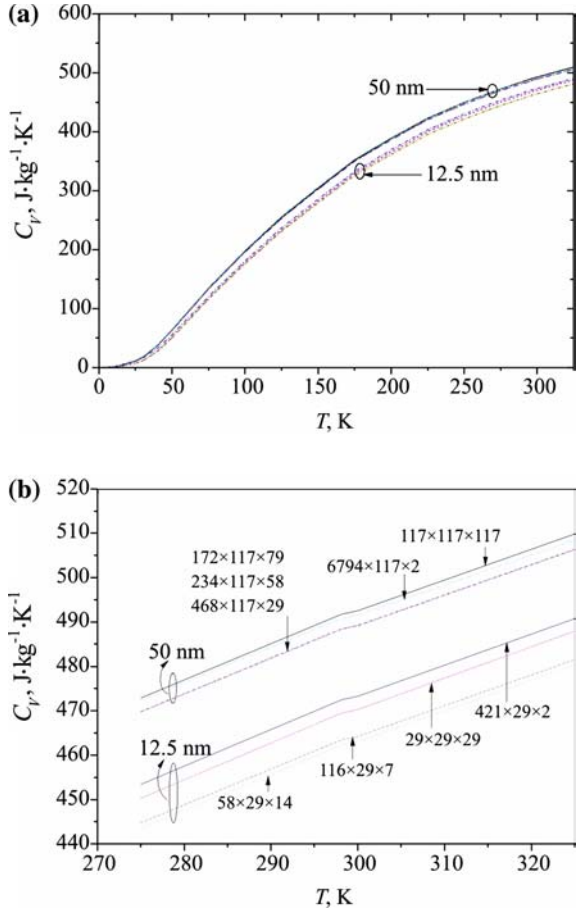

Fig. 4. Effect of particle shape on the specific heat capacity of 50 nm and 12.5 nm CuO.

other types with the data appearing almost on a similar curve. This is different from the conclusion of Prasher and Phelan [11] on aluminum and rutile. One possible explanation for this divergence is that the atom structure can greatly influence the size effect on the specific heat capacity. The other explanation for it is that the magnetic specific heat capacity will become important for copper oxide. For the convenience of understanding, the following analysis will not consider the particle shape effect on the specific heat capacity of CuO nanocrystals, and we will take the cubical crystal as a sample.

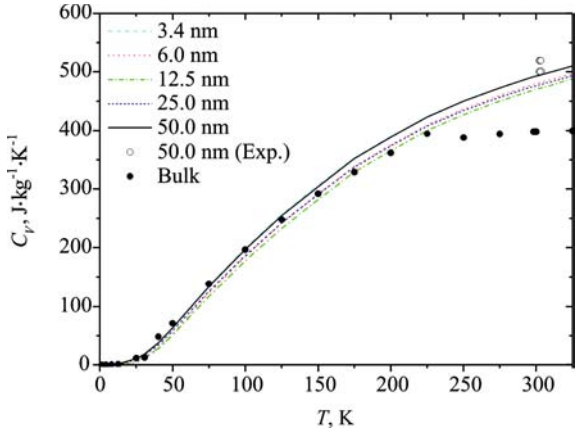

Fig. 5. Size effect on specific heat capacity of CuO.

4.2. Effect of Particle Size

The variation of the specific heat capacity of nanoparticles with temperature is shown in Fig. 5, where the bulk value is calculated from the specific heat capacity at constant volume, reported in Ref. 15, using the relation between specific heat capacity at constant volume and its corresponding result at constant pressure. It can be seen that, in the high-temperature region, the specific heat capacity of a CuO crystal is obviously higher than the bulk value; while in the low-temperature region, the specific heat capacity of a nanoparticle is lower than the bulk value. Between these two regions, there exists a transforming relation for the specific heat capacity of a CuO nanoparticle. Figure 6 shows the size effect on the specific heat capacity of a CuO nanoparticle in the high-temperature region. It seems that the different temperature regions give different relations between the particle size and specific heat capacity, in addition to the monotonic decrease relation proposed by Prasher and Phelan [11]. In the high-temperature region, the size effect on the specific heat capacity show an irregular behavior, which decreases monotonically and then increases with temperature in different areas, as shown in Fig. 6; the monotonic decrease relation only exists in the low-temperature region, as shown in Fig. 7. This may be related to the incidence of both the quantum effect and size effect on the specific heat capacity of a CuO nanoparticle.

For nanoparticles larger than 10 nm, the quantum effect can be neglected, and the specific heat capacity will decrease monotonically with the diameter of a nanoparticle due to the size effect. While for a nanoparticle that is smaller than 10 nm, the quantum effect will increase the spe-

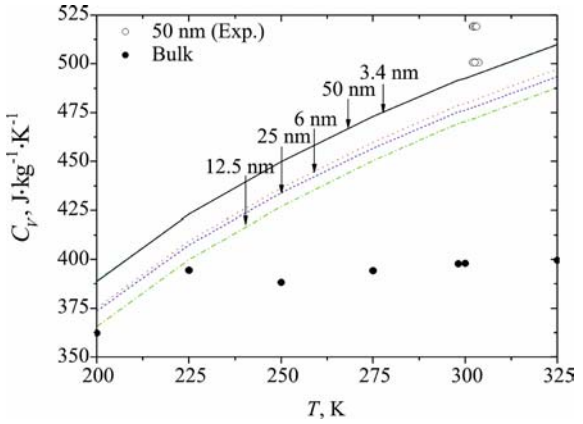

Fig. 6. Size effect on specific heat capacity of CuO (high temperature).

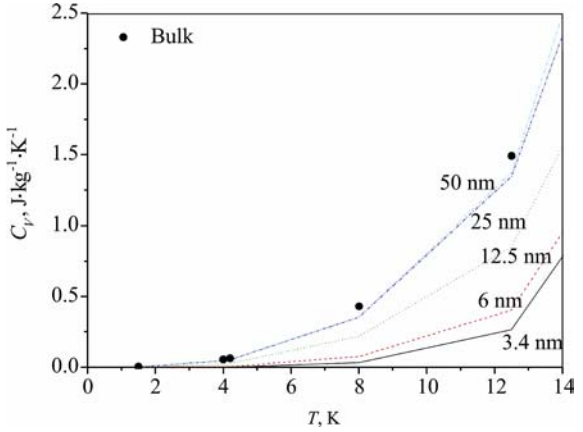

Fig. 7. Size effect on specific heat capacity of CuO (low temperature).

cific heat capacity of a nanoparticle uniformly, and thus create the irregular behavior phenomenon. Also, Figs. 5 and 6 show the averaged value of the specific heat capacity of a 50 nm CuO nanoparticle at room temperature, using the so-called quasi-steady-state method to measure the effective specific heat capacity of a CuO-water nanofluid with a possible uncertainty within 4.3% [2], and deducted the experimental data of a CuO nanoparticle. The calculated results show that the model for predicting the specific heat capacity of a CuO nanoparticle fits quite well with experimental data at temperatures below 225 K. An obvious increase of the

specific heat capacity for a nanoparticle can be observed in our experiment near 300 K from Figs. 5 and 6.

4.3. Nondimensionalization of Size Effect

From the above-mentioned discussion, it can be seen that the dimensionless variable, R, proposed by Prasher and Phelan [11] will not be suitable for predicting the specific heat capacity of a CuO nanoparticle. Comparing Eqs. (8) and (12)–(14), a novel dimensionless variable can be proposed as

$$R^* = \frac{Nk_B}{d^3T^2}. \tag{15}$$

The new dimensionless variable may be more generalized than R, since it has considered all the related factors, that is the size, temperature, numbers of primitive cells, etc. Figure 8 shows the variation of the dimensionless specific heat capacity of a CuO nanoparticle, $C_V/C_{V,\mathrm{Bulk}}$, with R^*, where $C_{V,\mathrm{Bulk}}$ is the bulk specific heat capacity at constant volume. It can be seen that the specific heat capacity of CuO nanoparticles of different diameters fit well with the analytical fitting curve. Of course, its universality needs to be checked with experiments at higher temperatures and with other kinds of nanoparticles.

5. CONCLUSIONS

In this paper, we have treated the different contributions of surface and interior atoms to the specific heat capacity of a nanoparticle and

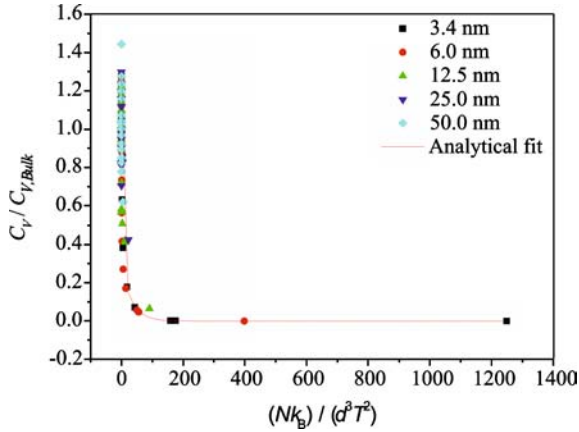

Fig. 8. Nondimensional relation of specific heat capacity.

calculated the specific heat capacity of a nanoparticle with the Einstein and Debye models, to study the size and surface effects on the specific heat capacity, while using the elastic continuum assumption. The effect of size and temperature and the softening of surface atom vibrations were studied, and a new dimensionless variable was proposed to characterize the effect of particle size and temperature on the specific heat capacity. The proposed model was used to fit experimental data for CuO nanoparticles. It shows that this model fits well with related experimental data. Further work is necessary to check the universality for higher temperatures and for other nanoparticles.

ACKNOWLEDGMENTS

This work was financially supported by the National Natural Science Foundation of China (Grant No. 59995550-3).

REFERENCES

1. P. Kebblinski, S. R. Philipot, S. U. S. Choi, and J. A. Eastman, *Int. J. Heat Mass Transfer* **45**:855 (2002).
2. L. P. Zhou and B. X. Wang, *Chinese J. Eng Thermophys.* **24**:1037 (2003). [in Chinese]
3. M. Planck, *Theorie de Warmestrahlung*, 6th Ed. (Joh. Ambrosius Barth, Leipzig, 1921).
4. G. Jura and K. S. Pitzer, *J. Am. Chem. Soc*. **74**: 6030 (1952).
5. V. Novotny, P. P. M. Meincke, and J. H. P. Watson, *Phys. Rev. Lett*. **28**:901 (1972).
6. H. P. Baltes and E. R. Hilf, *Solid State Commun*. **12**:369 (1973).
7. R. Lautenschleger, *Solid State Commun*. **16**:1331 (1975).
8. G. H. Comsa, D. Heitkamp, and H. S. Rade, *Solid State Commun.* **24**:547 (1977).
9. N. Nishiguchi and T. Sakuma, *Solid State Commun.* **38**:1073 (1981).
10. H. Z. Zhang and J. F. Banfield, *NanoStructured Materials* **10**:185 (1998).
11. R. S. Prasher and P. E. Phelan, Int. J. Heat Mass Transfer **42**:1991 (1999).
12. C. Kittel, *Introduction to Solid State Physics*, 5th Ed. (Wiley, New York, 1986).
13. Z. J. Deng, Q. Sun, and Q. Wang, *Ultrafine Particles and Fractals* (Southwest Normal University, Chongqing, China, 1993). [in Chinese]
14. S. Asbrink and L.-J. Norrby, *Acta Crystallogr*. B **26**:8 (1970).
15. A. Junod, D. Eckert, G. Triscone, J. Muller, and W. Reichard, *J. Phys., Condens. Matter* **1**:8021 (1989).